Anal Bioanal Chem (2008) 390:317–322
DOI 10.1007/s00216-007-1710-4

SHORT COMMUNICATION

Detection of molecular processes in the intact retina by ATR-FTIR spectromicroscopy

Sebastiano Massaro · Theodora Zlateva · Vincent Torre · Luca Quaroni

Received: 18 August 2007 / Revised: 10 October 2007 / Accepted: 16 October 2007 / Published online: 9 November 2007

Abstract We used Fourier transform infrared spectromicroscopy in the attenuated total reflection configuration to study biochemical events associated with the response to light of an intact retina. We show that the technique is suitable for the detection in real time of molecular processes occurring in rod outer segments induced by light absorption. Two-dimensional correlation analysis was applied to the identification and interpretation of specific spectral changes associated to the evolution of the system. The technique allows us to observe an extensive protein translocation, which we interpret as arising from the release of transducin from the disk membrane and its redistribution from the outer segment towards the inner segment of rod cells. These results are in full agreement with our current understanding of retinal physiology and validate the technique as a useful tool for the study of complex molecular processes in intact tissue.

L. Quaroni
Sincrotrone Trieste,
34012 Basovizza,
Trieste, Italy

S. Massaro · T. Zlateva · V. Torre
International School for Advanced Studies (SISSA),
Via Beirut 2,
34024 Trieste, Italy

Present address:
L. Quaroni (✉)
Canadian Light Source,
Saskatoon, SK S7N 0X4, Canada
e-mail: Luca.Quaroni@lightsource.ca

Present address:
T. Zlateva
Department of Pathology and Laboratory Medicine,
University of Saskatchewan,
Saskatoon, SK S7N 0W8, Canada

Keywords Phototransduction · ATR-FTIR · Retina · Transducin · Rod cell

Introduction

Fourier transform infrared (FTIR) spectroscopy has been used for decades as a technique for characterizing the molecular properties of biological molecules, such as the presence of specific functional groups, geometrical properties, and more. The attenuated total reflection (ATR) optical configuration has permitted the application of FTIR spectroscopy to thick or layered samples. To date the bulk of applications of ATR spectroscopy in the biological field has been limited to relatively simple systems, such as purified proteins, lipid bilayers, nucleic acids, and simple mixtures of biopolymers. Applications to the study of complex cellular systems and tissue have been demonstrated. However, they normally consist of a static type of analysis, where the technique is used to study the presence and localization of specific molecular species in a tissue section [1]. In this work we demonstrate the capabilities of ATR in the spectromicroscopy configuration to study dynamic processes within the retina of amphibians and show that it is possible to probe some molecular events in an in-vivo preparation.

The retina is highly specialized tissue with a characteristic layered structure. Amphibian retinas are composed mostly of rod photoreceptors, with a minority of cone photoreceptors. Rod photoreceptors are composed of an inner segment (rod inner segment, RIS) and an outer segment (rod outer segment, ROS) containing the molecular machinery involved in phototransduction, i.e. conversion of the light absorbed by rhodopsin molecules into the closure of light-sensitive channels [2–7]. Amphibian ROS are cylinders 30–50 μm long and 4–7 μm in diameter, where the

membrane encloses a stack of disks. In the dark, cyclic guanosine monophosphate (cGMP) molecules keep light-sensitive channels open. Light absorbed by rhodopsin molecules, located on the disks, initiates an enzymatic cascade leading to the hydrolysis of cGMP and, therefore, to the closure of light-sensitive channels. This enzymatic cascade is controlled by a G-protein, usually referred to as transducin [8–10], and by a variety of other enzymes whose properties and function have been elucidated to some extent [11–13] in electrophysiological experiments and in biochemical assays in vitro. The localization of ROSs within the retina gives rise to a layer about 30–50 μm thick which comprises most of the molecular phototransduction machinery.

Experimental

FTIR spectromicroscopy measurements were performed using a Bruker (Bruker Optics, Billerica, MA, USA) Vertex 70 FTIR spectrometer coupled to a Hyperion 3000 IR microscope. A 20× ATR objective (Bruker Optics) with a germanium internal reflection element (IRE) was mounted on the microscope for use in micro-ATR experiments. The interferometer and microscope were purged with a constant flow of dry nitrogen gas. A KBr beamsplitter was used in the interferometer, together with an MCT microscope detector. One-hundred and twenty-eight scans were added for each measurement, using 4 cm^{-1} resolution. Interferograms were Fourier transformed without zero filling.

Data processing and 2D correlation analysis were performed using the software package Opus (Bruker Optics). Generalized 2D correlation analysis was based on the method developed by Noda et al. [14–18].

All chemicals were purchased from Sigma-Aldrich (St Louis, MO, USA) and were of the highest grade of purity available.

Retinas from the toad *Bufo regularis* were removed form dark-adapted (12 h) animals under dim light illumination [19–21]. After decapitation by means of a guillotine and pithing, eyes were enucleated. Dissection of the retina was accomplished under a stereo zoom dissection microscope. The eye was cut vertically and the resulting eyecup was dipped in a Petri dish containing Ringer's solution (NaCl 80 mmol L^{-1}, KCl 2 mmol L^{-1}, $CaCl_2$ 0.1 mmol L^{-1}, $MgSO_4$ 0.1 mmol L^{-1}, NaH_2PO_4/Na_2HPO_4 12.5 mmol L^{-1}). The retina was gently grasped using small forceps and removed from the sclera and the pigment epithelium. Freshly dissected retinas were rinsed gently in Ringer's solution and transferred, photoreceptor side up, on to a sample holder that kept the retina constantly immersed in the solution. Under these conditions the retinas remain responsive to light for many hours as long as exposure to intense light is avoided [21].

Dark-adapted retinas were deposited on the bottom of a sample holder plate, covered with a drop of Ringer's solution and centered on the microscope stage under the crystal. Optical contact between the retina and the crystal was achieved by slowly lifting the microscope stage until the detection system of the objective indicates full alignment. The dynamometer in the objective is set so that the minimum force setting (0.5 N) is selected. All operations were performed under a dim red light.

A Uvico metal halide lamp (Rapp OptoElectronic, Hamburg, Germany) was used for sample illumination. The retina was stimulated for 60 s with 130 mW cm^{-2} of green (540 nm) light.

Results

We performed micro ATR measurements by placing retinal tissue in contact with the germanium IRE from the ROS side. Because of the geometry of the experiment, the evanescent field from the internally reflected beam extends 1 or 2 μm beyond the crystal-sample interface, into the ROS themselves, allowing spectroscopic measurements on a region of about one hundred disks.

After allowing a few minutes for the retina to stabilize, we recorded several spectra of the outer segments, in the dark, until the system was mechanically and thermally stable and no spectral changes were observed. We then stimulated the retina for 60 s with a green light delivering approximately 100 Lux. Evolution of the system was studied by collecting spectra every 30 s for 30 min or longer. Spectral changes are reported as difference spectra relative to the last spectrum recorded before illumination (Figs. 1a and b).

Twenty measurements were performed. We discarded those where damage to the retina was obvious (perforation of the retina) and those where no coloring of the retina was observed after illumination (indicating that no photoresponse had occurred and the retina was not functional). This leaves six measurements where the observed processes were reproduced.

Illumination induced changes in the spectral region of amide and carbonyl absorption bands over a time scale of several minutes. The dominant changes in this region correspond to the decrease of an apparent doublet around 1620 cm^{-1} and 1555 cm^{-1} and the increase of an apparent doublet around 1650 cm^{-1} and 1540 cm^{-1}. Additional changes are observed for the ester carbonyl band at 1745 cm^{-1}, phosphate bands at 1147 cm^{-1} and 1201 cm^{-1}, and other bands, possibly from methylene and amide vibrations, at 1348 cm^{-1} and 1444 cm^{-1}. Other major changes are a decrease in the absorption of the water and hydroxyl band at 3400 cm^{-1} and an increase of methyl and methylene

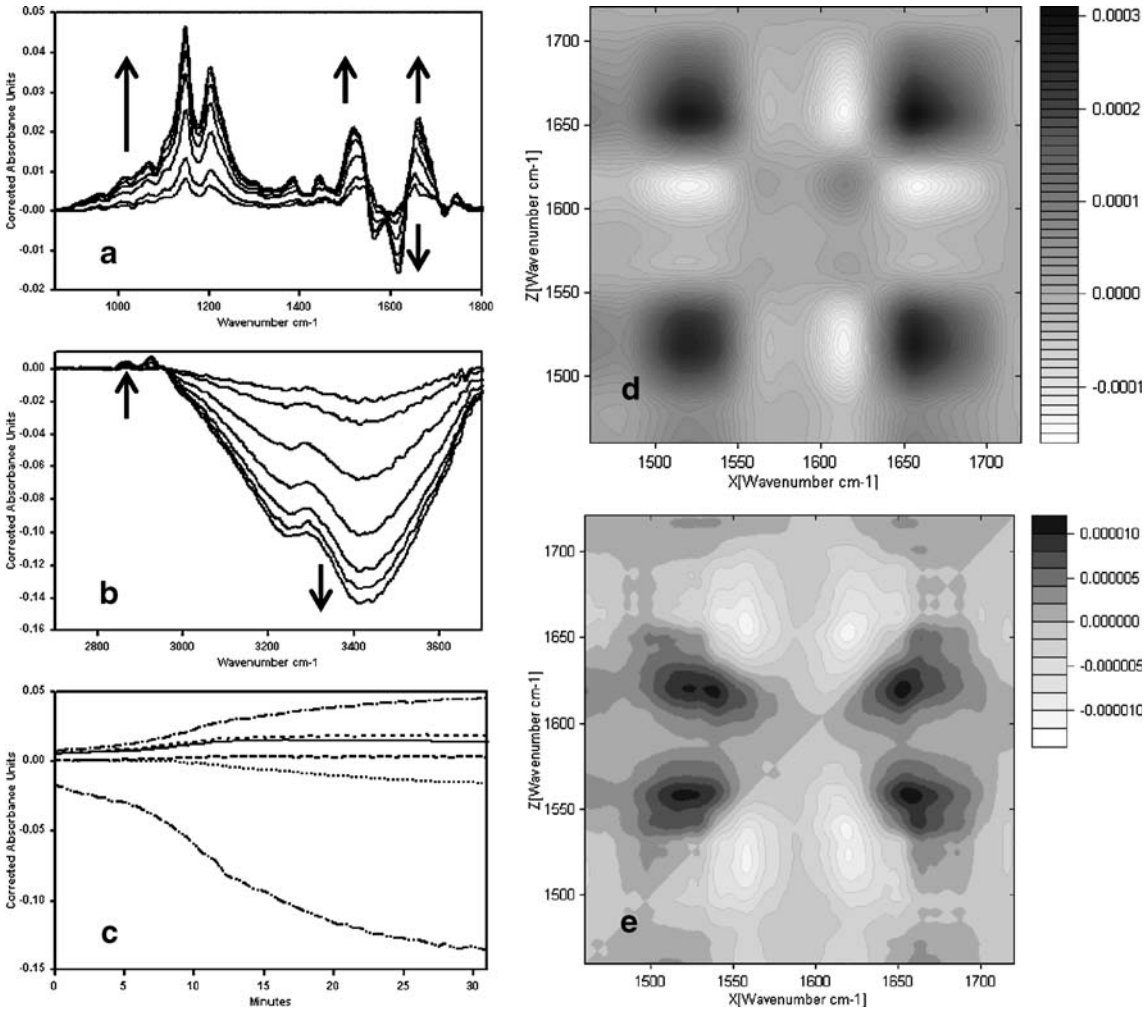

Fig. 1 **a**. Differential changes in absorption in the 860 cm^{-1}–1800 cm^{-1} spectral region after illumination. Spectra are reported as differences from the spectrum before illumination and recorded at 5-min intervals. **b**. Differential changes in absorption in the water and alkyl spectral region after illumination. Spectra are reported as differences from the spectrum before illumination and recorded at 5-min intervals. **c**. Time course of the differential changes in absorption at various wavelengths after illumination: from bottom to top, 3422 cm^{-1}, 1513 cm^{-1}, 1619 cm^{-1}, 1748 cm^{-1}, 1536 cm^{-1}, 1655 cm^{-1}, 1150 cm^{-1}. **d**. Synchronous correlation plot of the differential spectral variations in the 1450–1750 cm^{-1} region. **e**. Asynchronous correlation plot of the differential spectral variations in the 1450–1750 cm^{-1} region

stretching vibrations around 2900 cm^{-1}. Changes develop over a period of approximately 30 min, after which time the system stabilizes (Fig. 1c).

Some differences were observed in repeated experiments. These amounted to relative intensity of band variations for chromophore A and chromophore B. The spectra shown in this article were selected among those that display comparable amplitude changes for chromophore A and chromophore B, which was the most common situation.

Excessive pressure by the crystal appears to damage the retina. We assume that this is due to rupture of the rod cells at the cilium between outer and inner segment (it is not uncommon for rod cells to rupture at this position under mechanical stress). If a measurement is taken while applying increasing pressure, changes qualitatively similar to those seen upon photostimulation are observed, presumably because of release of cytoplasm components into the solution. For this reason waiting for stabilization is essential after placing the retina in contact with the crystal.

Two-dimensional (2D) correlation analysis of the sequence of difference spectra was used to extract information from the system in the amide spectral region. Interpretation of 2D correlation spectra is an established technique of data analysis and has been discussed in detail in the literature [14–18]. It is based on the conversion of a set of spectral changes as a function of time (or any other parameter that is subject to change) into a pair of 2D spectra known as the synchronous and asynchronous spectra.

The synchronous spectrum identifies all pairs of spectral peaks that are changing in synchrony, either with the same

or with opposite phase. The asynchronous spectrum identifies all pairs of peaks that are changing without being in synchrony. In addition, it provides information on the relative sequence of spectral changes. Joint analysis of both synchronous and asynchronous spectra permits the unravelling of sequential events in complex spectra containing multiple chromophores with similar but not identical time evolution.

The synchronous correlation plot is shown in Fig. 1d. It identifies all dominant spectral components that are subject to dynamic changes. In addition, spreading of peaks in the second dimension enables resolution of weaker components, which are not obvious from direct observation of one-dimensional spectra. This reveals that the peak close to 1540 cm^{-1} is actually a doublet, with a component at about 1525 cm^{-1} and another component at 1540 cm^{-1}. Similarly a multiplet is partially resolved at higher frequency, with a major component at 1655 cm^{-1} and minor components around 1645 cm^{-1} and 1665 cm^{-1}. Positive cross-correlation peaks indicate that the peak around 1650 cm^{-1} and the doublet around 1540 cm^{-1} are changing in phase. The same is true for the pair around 1620 cm^{-1} and 1555 cm^{-1}. Negative cross-correlation peaks indicate changes that occur with opposite phase, i.e. one component increases in synchrony with the decrease of another component. Negative cross-correlation peaks are observed around 1655 cm^{-1} and 1620 cm^{-1}. Negative peaks are also observed for the doublet around 1540 cm^{-1} and the peak around 1555 cm^{-1}.

The asynchronous correlation plot (Fig. 1e) reveals spectral changes that occur with a phase difference which is neither 0 nor π [14–18]. In general, the asynchronous plot provides better resolution of overlapping components than the synchronous plot, allowing identification of additional spectral peaks and more accurate positioning. The peaks reported above can be clearly observed at 1664, 1653, 1647, 1620, 1558, 1543, 1537, and 1524 cm^{-1}.

The pair of peaks at 1620 cm^{-1} and 1558 cm^{-1} displays synchronous correlation. However no corresponding cross peaks are observed in the asynchronous spectrum. This indicates that intensity variations of the two bands are completely and exclusively in phase, as expected for bands arising from the same chromophore. This relationship, together with the observed peak positions indicate that the two bands can be assigned to an Amide I/Amide II pair from the same chromophore. The same conclusions can be drawn for the triplet at 1653 cm^{-1} (Amide I), 1537 cm^{-1}, and 1524 cm^{-1} (both Amide II components). We call the two species involved chromophore A (1620 cm^{-1} and 1558 cm^{-1}) and chromophore B (1653 cm^{-1}, 1537 cm^{-1}, and 1524 cm^{-1}).

The asynchronous spectrum also shows weaker cross-correlation peaks, indicating the presence of minor components that absorb at 1664 cm^{-1}, 1647 cm^{-1}, and 1543 cm^{-1}, which go undetected without the application of 2D correlation analysis. The peak at 1647 cm^{-1} is likely due to the bending vibration of water. A decrease in the stretching absorptions of water is clearly observed above 3000 cm^{-1} in Fig. 1b and a corresponding variation must occur for the bending mode. The other peaks could also arise from polypeptide chromophores and be assigned to additional Amide I and Amide II vibrations. However, their weakness and small relative contribution prevents us from carrying out the assignment as done in the previous paragraph.

The asynchronous correlation spectrum allows us to identify the sequence of events occurring after photostimulation [14–18]. Table 1 reports the analysis for the spectral components of chromophores A and B. The observed pattern is fully consistent with a sequence in which changes in chromophore A precede changes in chromophore B.

2D correlation analysis over the whole MidIR spectral region (data not shown) indicates that variation of chromophore B occurs in synchrony with all the other major changes observed in the spectrum, namely the increase of bands at 1147 cm^{-1} and 1201 cm^{-1}, assigned to phosphate headgroups in phospholipids, and the decrease of the water band at about 3400 cm^{-1}. The variation of chromophore A precedes all other variations.

Discussion

Light-induced changes of IR absorption spectra can provide important clues on the biochemical events occurring inside at the tip of ROS, probed by the evanescent wave at the crystal-sample interface.

Extensive FTIR and ATR studies have been carried out on the structural changes induced in rhodopsin by photostimulation [19–24]. These studies addressed events on a time scale faster than 1 s, ranging from the conformational conversion of retinal to the inter-conversion between the various conformational intermediates of rhodopsin. These events give rise to changes of the order of 10^{-3} absorbance units in preparations that are at least as concentrated as the ROS. The absorbance changes we observe in our measurements are at least one order of magnitude larger, too large to be interpreted as light-induced conformational changes of rhodopsin. Furthermore, they occur on time scales that are much slower, ranging from 30 s to 30 min. Therefore, the changes in Fig. 1 are likely to arise from different processes.

The doublet at 1630 cm^{-1} and 1530 cm^{-1}, corresponding to chromophore A, can be assigned to the Amide I and Amide II bands of a protein. The major protein components in dark-adapted ROS are the proteins rhodopsin (estimated to be about 5 mmol L^{-1} in concentration) and transducin (estimated at about 0.5 mmol L^{-1}). Both are present at concentrations detectable by IR absorption spectroscopy,

Table 1 Assignment of the sequence of spectral changes from the asynchronous plot

X (cm^{-1})	Y (cm^{-1})	Asynchronous peak sign	Synchronous peak sign	Sequential change in coordinate	Sequential change in chromophore concentration
1620	1558	NA	+	NA	NA
1653	1537	NA	+	NA	NA
1653	1524	NA	+	NA	NA
1620	1537	−	−	X < Y	A < B
1620	1524	−	−	X < Y	A < B
1653	1558	+	−	Y < X	A < B
1653	1620	+	−	Y < X	A < B

X and Y indicate the coordinates of a cross-correlation peak in the asynchronous plot. Peak signs indicate whether the cross-correlation peaks are positive (+), negative (−) or missing (NA). "Sequential change in coordinate" indicates which of the frequencies X and Y changes first. "Sequential change in chromophore concentration" identifies the chromophore (A or B) the concentration of which is changing first

although rhodopsin dominates the absolute absorption spectrum. The Amide I and II bands of the unknown chromophore are characteristic of a protein whose secondary structure is primarily β-sheet, consistent with an assignment to transducin. Experiments performed by Fahmy [28] have reported the variations observed in ATR spectra of a preparation of purified disk membranes upon release of transducin induced by a chemical stimulus. The main change is a decrease in intensity of an Amide I and II doublet with band positions characteristic of a β-sheet protein. The change appears to be fully developed after 30 min. The decrease is because membrane-free transducin diffuses into bulk buffer solution, thus leaving the evanescent field of the IRE. A similar experimental geometry is realized in our experiment, where the proximity to the IRE of the disks within the outer segment implies that a release of transducin from the disks and its relocation towards the inner segment would also give rise to a similar spectral change. Furthermore the time evolution reported by Fahmy is the same as we observe for changes we assign to chromophore A. The overall absorbance change, about 10^{-2} AU in 30 min, is also comparable and is of magnitude consistent with an extensive loss of transducin from the outer segment. Overall these observations support the assignment of chromophore A to transducin. The observed decrease in transducin absorbance can be interpreted as a decrease in the concentration of transducin in the outer tip of ROS.

The extensive translocation of transducin from the ROS towards the inner segment under conditions of intense illumination is known. The translocation has already been observed in immunofluorescence experiments [29–34]. The effect is explained as a protective response of rod cells, aimed at shutting off the phototransduction cascade under conditions of intense illumination [35].

The Amide I and II bands of chromophore B are characteristic of an α-helix protein, consistent with an assignment to rhodopsin [5]. The bands of chromophore B increase in phase with bands assigned to lipid membrane components. Rhodopsin is an intrinsic protein associated with both disk and cytoplasmic membrane and, as such, is restricted from freely migrating within the outer segment. The synchrony between changes in lipid absorption bands and chromophore B bands is consistent with the association of the latter with ROS membranes, in turn supporting the identification of chromophore B with rhodopsin. The observed changes indicate an increase in local concentration of both rhodopsin and the associated membranes in the proximity of the crystal surface. This is most likely ascribed to a compression of disk membranes against the crystal surface. The interpretation is fully supported by the observed parallel decrease of water absorption bands, indicating expulsion of water, either from the interstitial space between disks or from the luminal space within disks.

The final decrease of absorption attributed to transducin is approximately 10% of the total initial absorbance of the Amide I band. This is comparable to the abundance of transducin relative to rhodopsin, suggesting that most of the transducin initially present is lost from the portion of the outer segment within the evanescent field.

The degree of water expulsion and disk compression cannot be estimated accurately. Lipids, water, and rhodopsin are the most abundant components of ROS and are expected to provide the dominant contributions to the ATR spectrum. Therefore, the observed variations can arise from a relatively small reorganization within the ROS.

Conclusions

We have shown that several molecular aspects of the process of phototransduction can be studied ex vivo by using a micro ATR configuration. Overall the data indicate a process in which a β-sheet rich protein, presumably transducin, is expelled from the interstitial space between disks after exposure to light and migrates away from the ROS [31–34]. Its expulsion is followed by a compression

of the disks within the ROS and reduction of water content. These conclusions are in agreement with our current understanding of retinal physiology, thus providing full validation of the technique.

References

1. Kazarian SG, Chan KLA (2006) Biochim Biophys Acta 1758:858–867
2. Schnapf JL, Baylor DL (1987) Sci Am 256:40–47
3. Baylor D (1996) Proc Nat Acad Sci 93:560–565
4. Forti S, Menini A, Rispoli G, Torre V (1989) J Physiol 419:265–295
5. Menon ST, Han M, Sakmar TP (2001) Physiol Rev 81:1659–1688
6. Kramer RH, Molokanova E (2001) J Exp Biol 204:2921–2931
7. Hamer RD, Nicholas SC, Tranchina D, Lamb TD, Jarvinen JL (2005) Vis Neurosci 22:417–436
8. Flaherty KM, Zozulya S, Stryer L, McKay DB (1993) Cell 75:709–716
9. Stryer L (1996) Proc Nat Acad Sci 93:557–559
10. Wall MA, Coleman DE, Lee E, Iniguez-Lluhi JA, Posner BA, Gilman AG, Sprang SR (1995) Cell 83:1047–1058
11. Palczewski K (ed) (2003) Vertebrate phototransduction and the visual cycle. Academic Press, New York
12. Maeda T, Imanishi Y, Palczewski K (2003) Prog Retin Eye Res 22:417–434
13. Lamb TD, Pugh EN Jr (2004) Prog Retin Eye Res 23:307–380
14. Noda I (1989) J Am Chem Soc 111:8116–8118
15. Noda I (1990) Appl Spectrosc 44:550–561
16. Noda I (1993) Appl Spectrosc 47:1329–1336
17. Noda I (2007) Anal Sci 23:139–146
18. Marcott C, Dowrey AE, Noda I (1994) Anal Chem 66:1065A
19. Fahmy K, Sakmar TP, Siebert F (2000) Methods Enzymol 315: 178–196
20. Fahmy K, Jager F, Beck M, Zvyaga TA, Sakmar TP, Siebert F (1993) Proc Natl Acad Sci USA 90:10206–10210
21. Jager F, Fahmy K, Sakmar TP, Siebert F (1994) Biochemistry 33:10878–10882
22. Rath P, Decaluwe Ll, Bovee-Geurts PH, Degrip WJ, Rothschild KJ (1993) Biochemistry 32:10277–10282
23. Rothschild KJ (1992) J Bioenerg Biomembr 24:147–167
24. Siebert F (1995) Israel J Chem 35:309–323
25. Lolley RN (1982) In Packer L (ed) Methods Enzymol, Biomembranes, Part H:37–39
26. Baumann C (1982) In Packer L (ed) Methods Enzymol, Biomembranes, Part H:29–34
27. Newman EA, Bartosch R (1999) J Neurosci Meth 93:169–175
28. Fahmy K (1998) Biophys J 75:1306–1318
29. Sokolov M, Lyubarsky AL, Strissel KJ, Savchenko AB, Govardovskii VI, Pugh EN Jr, Arshavsky VY (2002) Neuron 33:95–106
30. Peterson JJ, Tam BM, Moritz OL, Shelamer CL, Dugger DR, McDowell JH, Hargrave PA, Papermaster DS, Smith WC (2003) Exp Eye Res 76:553–563
31. Brann MR, Cohen LV (1987) Science 235:585–587
32. Zhu X, Li A, Brown B, Weiss ER, Osawa S, Craft CM (2002) Mol Vis 8:462–471
33. Nair KS, Hanson SM, Mendez A, Gurevich EV, Kennedy MJ, Shestopalov VI, Vishnivetskiy SA, Chen J, Hurley JB, Gurevich VV, Slepak VZ (2005) Neuron 46:555–567
34. Elias RV, Sezate SS, Cao W, McGinnis JF (2004) Mol Vis 10:672–681
35. Fain GL (2006) Bioessays 28:344–354